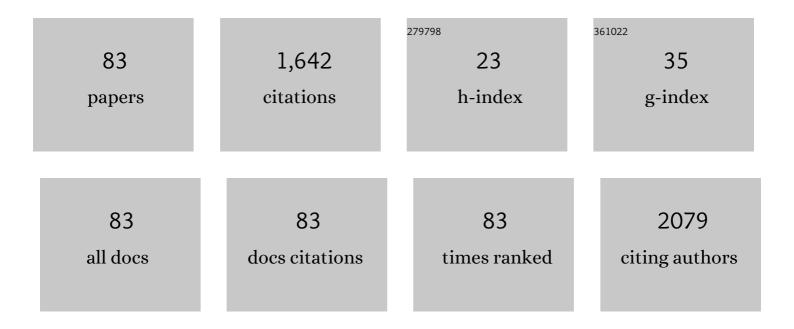
Ryoma HAYAKAWA

List of Publications by Year in descending order

Source: https://exaly.com/author-pdf/3086110/publications.pdf Version: 2024-02-01



#	Article	IF	CITATIONS
1	Multi-Valued Logic Circuits Based on Organic Anti-ambipolar Transistors. Nano Letters, 2018, 18, 4355-4359.	9.1	102
2	Recent progress in photoactive organic field-effect transistors. Science and Technology of Advanced Materials, 2014, 15, 024202.	6.1	80
3	Optically and Electrically Driven Organic Thin Film Transistors with Diarylethene Photochromic Channel Layers. ACS Applied Materials & Interfaces, 2013, 5, 3625-3630.	8.0	78
4	Large Magnetoresistance in Single-Radical Molecular Junctions. Nano Letters, 2016, 16, 4960-4967.	9.1	75
5	Negative Differential Resistance Transistor with Organic pâ€n Heterojunction. Advanced Electronic Materials, 2017, 3, 1700106.	5.1	57
6	Optical switching of carrier transport in polymeric transistors with photochromic spiropyran molecules. Journal of Materials Chemistry C, 2013, 1, 3012.	5.5	56
7	Antiambipolar Transistor: A Newcomer for Future Flexible Electronics. Advanced Functional Materials, 2020, 30, 1903724.	14.9	50
8	Photochromism for optically functionalized organic field-effect transistors: a comprehensive review. Journal of Materials Chemistry C, 2020, 8, 10956-10974.	5.5	48
9	Shot Noise of 1,4-Benzenedithiol Single-Molecule Junctions. Nano Letters, 2016, 16, 1803-1807.	9.1	44
10	Demonstration of diamond field effect transistors by AlN/diamond heterostructure. Physica Status Solidi - Rapid Research Letters, 2011, 5, 125-127.	2.4	39
11	Laser Patterning of Optically Reconfigurable Transistor Channels in a Photochromic Diarylethene Layer. Nano Letters, 2016, 16, 7474-7480.	9.1	38
12	Self-Assembled Molecular Nanowires of 6,13-Bis(methylthio)pentacene: Growth, Electrical Properties, and Applications. Nano Letters, 2008, 8, 3273-3277.	9.1	36
13	Continuous hydrothermal synthesis of nickel oxide nanoplates and their use as nanoinks for p-type channel material in a bottom-gate field-effect transistor. Nanotechnology, 2010, 21, 134009.	2.6	36
14	Unique Device Operations by Combining Optical-Memory Effect and Electrical-Gate Modulation in a Photochromism-Based Dual-Gate Transistor. ACS Applied Materials & Interfaces, 2013, 5, 9726-9731.	8.0	35
15	Device Geometry Engineering for Controlling Organic Antiambipolar Transistor Properties. Journal of Physical Chemistry C, 2018, 122, 6943-6946.	3.1	35
16	Interface Engineering for Controlling Device Properties of Organic Antiambipolar Transistors. ACS Applied Materials & Interfaces, 2018, 10, 2762-2767.	8.0	32
17	Development of AlN/diamond heterojunction field effect transistors. Diamond and Related Materials, 2012, 24, 206-209.	3.9	31
18	Fundamentals of Organic Antiâ€Ambipolar Ternary Inverters. Advanced Electronic Materials, 2020, 6, 1901200.	5.1	31

#	Article	IF	CITATIONS
19	Early Stage of Growth of a Perylene Diimide Derivative Thin Film Growth on Various Si(001) Substrates. Journal of Physical Chemistry C, 2007, 111, 12747-12751.	3.1	29
20	Perspective: Highly ordered MoS2 thin films grown by multi-step chemical vapor deposition process. APL Materials, 2016, 4, .	5.1	28
21	Enhanced Quantum Efficiency in Vertical Mixed-Thickness <i>n</i> -ReS ₂ / <i>p</i> -Si Heterojunction Photodiodes. ACS Photonics, 2019, 6, 2277-2286.	6.6	26
22	Energy-level alignments and photo-induced carrier processes at the heteromolecular interface of quaterrylene and N,N′-dioctyl-3,4,9,10-perylenedicarboximide. Physical Chemistry Chemical Physics, 2011, 13, 6280.	2.8	25
23	Optically Controllable Dual-Gate Organic Transistor Produced via Phase Separation between Polymer Semiconductor and Photochromic Spiropyran Molecules. ACS Applied Materials & Interfaces, 2014, 6, 10415-10420.	8.0	23
24	Interface engineering for improving optical switching in a diarylethene-channel transistor. Organic Electronics, 2015, 21, 149-154.	2.6	22
25	Carrier transport properties of MoS2 field-effect transistors produced by multi-step chemical vapor deposition method. Journal of Applied Physics, 2017, 121, .	2.5	22
26	Organic heterojunction transistors for mechanically flexible multivalued logic circuits. Applied Physics Express, 2021, 14, 081004.	2.4	22
27	Singleâ€Electron Tunneling through Molecular Quantum Dots in a Metalâ€Insulatorâ€Semiconductor Structure. Advanced Functional Materials, 2011, 21, 2933-2937.	14.9	21
28	Hard x-ray photoelectron spectroscopy study on band alignment at poly(3,4-ethylenedioxythiophene):poly(styrenesulfonate)/ZnO interface. Applied Physics Letters, 2012, 101, .	3.3	21
29	Analysis of nitrogen plasma generated by a pulsed plasma system near atmospheric pressure. Journal of Applied Physics, 2004, 96, 6094-6096.	2.5	19
30	Interface structure and the chemical states of Pt film on polar-ZnO single crystal. Applied Physics Letters, 2009, 94, 221904.	3.3	18
31	Enhanced Selectivity in Volatile Organic Compound Gas Sensors Based on ReS ₂ -FETs under Light-Assisted and Gate-Bias Tunable Operation. ACS Applied Materials & Interfaces, 2021, 13, 43030-43038.	8.0	18
32	Interface engineering for molecular alignment and device performance of quaterrylene thin films. Applied Physics Letters, 2008, 93, .	3.3	17
33	Growth and electrical properties of N,N′-bis(n-pentyl)terrylene- 3,4:11,12-tetracarboximide thin films. Applied Physics Letters, 2008, 92, 163301.	3.3	17
34	Enhanced Electrical Conductivity in Poly(3-hexylthiophene)/Fluorinated Tetracyanoquinodimethane Nanowires Grown with a Porous Alumina Template. Langmuir, 2013, 29, 7266-7270.	3.5	17
35	Electrically Reconfigurable Organic Logic Gates: A Promising Perspective on a Dualâ€Gate Antiambipolar Transistor. Advanced Materials, 2022, 34, e2109491.	21.0	17
36	Reaction of Si with excited nitrogen species in pure nitrogen plasma near atmospheric pressure. Thin Solid Films, 2006, 506-507, 423-426.	1.8	16

#	Article	IF	CITATIONS
37	Growth of quaterrylene thin films on a silicon dioxide surface using vacuum deposition. Organic Electronics, 2007, 8, 631-634.	2.6	16
38	Structural characterization and transistor properties of thickness-controllable MoS2 thin films. Journal of Materials Science, 2019, 54, 7758-7767.	3.7	15
39	ReS ₂ /hâ€BN/Graphene Heterostructure Based Multifunctional Devices: Tunneling Diodes, FETs, Logic Gates, and Memory. Advanced Electronic Materials, 2021, 7, .	5.1	15
40	Detailed structural analysis and dielectric properties of silicon nitride film fabricated using pure nitrogen plasma generated near atmospheric pressure. Journal of Applied Physics, 2006, 100, 073710.	2.5	14
41	Strain-effect for controlled growth mode and well-ordered structure of quaterrylene thin films. Journal of Chemical Physics, 2010, 133, 034706.	3.0	14
42	Ambipolar carrier transport in an optically controllable diarylethene thin film transistor. Organic Electronics, 2019, 64, 205-208.	2.6	14
43	Photoisomerization-Induced Manipulation of Single-Electron Tunneling for Novel Si-Based Optical Memory. ACS Applied Materials & Interfaces, 2013, 5, 11371-11376.	8.0	13
44	Organic-semiconductor nanoarchitectonics for multi-valued logic circuits with ideal transfer characteristics. Journal of Materials Chemistry C, 2021, 9, 15415-15421.	5.5	13
45	High-performance multivalued logic circuits based on optically tunable antiambipolar transistors. Journal of Materials Chemistry C, 2022, 10, 5559-5566.	5.5	13
46	Growth and structural characterization of molecular superlattice of quaterrylene and N,N′-dioctyl-3,4,9,10-perylenedicarboximide. Organic Electronics, 2009, 10, 1032-1036.	2.6	11
47	Stress Release Drives Growth Transition of Quaterrylene Thin Films on SiO ₂ Surfaces. Journal of Physical Chemistry C, 2009, 113, 2197-2199.	3.1	11
48	Ambipolar carrier transport in hetero-layered organic transistors consisting of quaterrylene and N,N′-dioctyl-3,4,9,10-perylenedicarboximide. Organic Electronics, 2011, 12, 1336-1340.	2.6	11
49	Evolution of Quaterrylene Thin Films on a Silicon Dioxide Surface Using an Ultraslow Deposition Technique. Journal of Physical Chemistry C, 2007, 111, 18703-18707.	3.1	10
50	Analysis of carrier transport in quaterrylene thin film transistors formed by ultraslow vacuum deposition. Journal of Applied Physics, 2008, 104, 024506.	2.5	10
51	Electrolyte-gated-organic field effect transistors functionalized by lipid monolayers with tunable pH sensitivity for sensor applications. Applied Physics Express, 2020, 13, 011005.	2.4	10
52	Structural analysis and transistor properties of hetero-molecular bilayers. Thin Solid Films, 2009, 518, 441-443.	1.8	9
53	Structural analysis and electrical properties of pure Ge3N4 dielectric layers formed by an atmospheric-pressure nitrogen plasma. Journal of Applied Physics, 2011, 110, 064103.	2.5	9
54	Stable operation of water-gated organic field-effect transistor depending on channel flatness, electrode metals and surface treatment. Japanese Journal of Applied Physics, 2019, 58, SDDH02.	1.5	9

#	Article	IF	CITATIONS
55	Multilevel Operation of Resonant Tunneling with Binary Molecules in a Metal–Insulator–Semiconductor Configuration. Journal of Physical Chemistry C, 2014, 118, 6467-6472.	3.1	8
56	Nanochannel effect in polymer nanowire transistor with highly aligned polymer chains. Applied Physics Letters, 2015, 106, .	3.3	8
57	P-type polymer-based Ag ₂ S atomic switch for "tug of war―operation. Japanese Journal of Applied Physics, 2017, 56, 06GF03.	1.5	8
58	Formation of Silicon Oxynitride Films with Low Leakage Current Using N2/O2Plasma near Atmospheric Pressure. Japanese Journal of Applied Physics, 2004, 43, 7853-7856.	1.5	7
59	Integration of molecular functions into Si device for nanoscale molecular devices. Thin Solid Films, 2014, 554, 2-7.	1.8	7
60	Soluble 2,6-Bis(4-pentylphenylethynyl)anthracene as a High Hole Mobility Semiconductor for Organic Field-effect Transistors. Chemistry Letters, 2016, 45, 1403-1405.	1.3	7
61	Photocontrollable ambipolar transistors with <i>ï€</i> -conjugated diarylethene photochromic channels. Japanese Journal of Applied Physics, 2019, 58, SDDH03.	1.5	7
62	Lightâ€Assisted and Gateâ€Tunable Oxygen Gas Sensor Based on Rhenium Disulfide Fieldâ€Effect Transistors. Physica Status Solidi - Rapid Research Letters, 2020, 14, 2000330.	2.4	7
63	Effect of Additional Oxygen on Formation of Silicon Oxynitride Using Nitrogen Plasma Generated near Atmospheric Pressure. Japanese Journal of Applied Physics, 2006, 45, 9025-9028.	1.5	6
64	The comparison of the growth models of silicon nitride ultrathin films fabricated using atmospheric pressure plasma and radio frequency plasma. Journal of Applied Physics, 2007, 101, 023513.	2.5	6
65	Schottky barrier height behavior of Pt–Ru alloy contacts on single-crystal n-ZnO. Journal of Applied Physics, 2010, 107, .	2.5	6
66	Layer-by-layer growth of precisely controlled hetero-molecular multi-layers and superlattice structures. Thin Solid Films, 2014, 554, 74-77.	1.8	6
67	Mn ₅ Ge ₃ C _{0.6} /Ge(1 1 1) Schottky contacts tuned by an n-ty ultra-shallow doping layer. Journal Physics D: Applied Physics, 2016, 49, 355101.	/pe 2.8	6
68	Polymer chain alignment and transistor properties of nanochannel-templated poly(3-hexylthiophene) nanowires. Journal of Applied Physics, 2016, 120, 055501.	2.5	6
69	Vertical resonant tunneling transistors with molecular quantum dots for large-scale integration. Nanoscale, 2017, 9, 11297-11302.	5.6	6
70	Variable temperature characterization of N,N′-Bis(n-pentyl)terrylene-3,4:11,12-tetracarboxylic diimide thin film transistor. Organic Electronics, 2009, 10, 1187-1190.	2.6	5
71	Impact of surface modification by addition of self-assembled monolayer for carrier transport of quaterrylene thin films. Thin Solid Films, 2009, 518, 437-440.	1.8	5
72	Photoelectron spectroscopic study on monolayer pentacene thin-film/polar ZnO single-crystal hybrid interface. Applied Physics Express, 2017, 10, 025702.	2.4	5

#	Article	IF	CITATIONS
73	Gate-bias tunable humidity sensors based on rhenium disulfide field-effect transistors. Japanese Journal of Applied Physics, 2021, 60, SBBH01.	1.5	5
74	Improved thermal stability in photochromism-based optically controllable organic thin film transistor. Organic Electronics, 2014, 15, 1891-1895.	2.6	4
75	Crystallographic polarity effect of ZnO on thin film growth of pentacene. Japanese Journal of Applied Physics, 2017, 56, 04CJ03.	1.5	4
76	On-terrace graphoepitaxy for remarkable one-dimensional growth of 2,7-dioctyl[1]benzothieno[3,2-b]benzothiophene (C8-BTBT) nanowires. Organic Electronics, 2019, 74, 33-36.	2.6	4
77	Single-charge transport through hybrid core–shell Au-ZnS quantum dots: a comprehensive analysis from a modified energy structure. Nanoscale, 2021, 13, 4978-4984.	5.6	3
78	Theoretical Insight into Quantum Transport Via Molecular Dots in a Vertical Tunnel Transistor. ACS Applied Electronic Materials, 2021, 3, 973-978.	4.3	3
79	Study of the exciton relaxation and recombination processes of a heteromolecular interface fabricated by a molecular superlattice growth technique. Chemical Physics Letters, 2011, 512, 227-230.	2.6	2
80	Molecular Alignment and Energy-Level Diagram at Heteromolecular Interface of Quaterrylene and Terrylene-3,4,11,12-Tetracarboximide. Journal of Nanoscience and Nanotechnology, 2011, 11, 4888-4892.	0.9	1
81	Potential of Directed- and Self-Assembled Molecular Nanowires for Optoelectronic Functional Devices. Japanese Journal of Applied Physics, 2012, 51, 06FA01.	1.5	1
82	Exciton dynamics at the heteromolecular interface between N,N′-dioctyl-3,4,9,10-perylenedicarboximide and quaterrylene, studied using time-resolved photoluminescence. AIP Advances, 2014, 4, 067112.	1.3	1
83	Fabrication of Silicon Nitride Film using Pure Nitrogen Plasma Generated near Atmospheric Pressure for III-V Semiconductor Fabrication. Materials Research Society Symposia Proceedings, 2004, 831, 144.	0.1	0